J. Water Environ. Nanotechnol., 4(4): 263-274 Autumn 2019

ORIGINAL RESEARCH PAPER

Decontamination study of Eriochrome Black-T from waste water by using AlTiPbO Nanoparticles (ATPO-NPs) for Sustainable Clean Environment

Ganesh Jethave[1], Umesh Fegade[2], Sanjay Attarde[1]* and Sopan Ingle[1]

[1]School of Environmental and Earth Sciences, KBC North Maharashtra University, Jalgaon, MS, India
[2]Bhusawal Arts, Science and P. O. Nahata Commerce College, Bhusawal, MS, India

Received: 2019-08-21 Accepted: 2019-10-18 Published: 2019-11-01

ABSTRACT

The successful synthesis and characterization of AlTiPbO Nanoparticles (ATPO-NPs) using a facile and straight forward co-precipitation method was reported in the present work. The detailed morphological characterization uncovered that the nanoparticles are of 28 nm in size. From the application perspective, the nanoparticles were utilized as a potential adsorbent to remove the toxic and hazardous dye from the aqueous phase. The point by point adsorption studies uncovered that the AlTiPbO nanoparticles made the Eriochrome black-T solution becomes colorless within 90 min. The outcome of the study verified by isotherms and kinetic study measurements and the adsorption system was examined. The nanoparticles have been effectively reused up to fifth cycle of the adsorption. A real sample analysis study revealed that ATPO-NPs could remove high concentrations (1000 mg/g) of dye from the industrial waste sample.

Keywords: *AlTiPbO nanoparticles, Decontamination, EBT Dye, Adsorption Mechanism*

How to cite this article
Jethave G, Fegade U, Attarde S, Ingle S. Decontamination study of Eriochrome Black-T from waste water by using AlTiPbO Nanoparticles (ATPO-NPs) for Sustainable Clean Environment. J. Water Environ. Nanotechnol., 2019; 4(4): 263-274.
DOI: 10.22090/jwent.2019.04.001

INTRODUCTION

The environment has become a significant concern for everyone, for the general public, business, scientific community, and researchers as well as policymakers at a domestic, European and global level, and especially for the issue of water contamination [1].

The use of different types of dyes in cosmetics, leather, paper, textile, and other industries is well-known. The release of unprocessed colored materials, especially organic dyes, from various manufacturing industries are the major threats to living organisms as the high extent of chemical, photolytic, and microbiological stabilities of such organic dyes are one of the most dangerous sources of water pollution [1, 2]. Dyes are difficult to remove in the environment, as the majority of them are stable and not light-degradable due to their complex structure. Most dyes are carcinogenic, toxic and mutagenic, in addition to having high-temperature stability, light and micro-organism attacks, making them stubborn compounds that lead to low quality and contamination by changing the content of COD and BOD in water [3b]. The incomplete degradation of such toxic dyes by aerobic methods cause significant annoyance in aquatic life and hence creates a dangerous threat to aquatic animals [3a, 4a]. Decontamination of industrial wastewater has become a top concern because of government demands for waste-free of pollutants to receiving water. This is a challenging and hard job. A universal technique for the removal of all contaminants from wastewater is also hard to identify. Among the many different procedures for processing wastewater, few are often used in industrial applications [4b]. Environmentalists

* Corresponding Author Email: *sb.attarde@yahoo.co.in*

have adopted different methodologies, for example, coagulation and flocculation, oxidation, film division, ultra-synthetic filtration, compound medicines, and adsorption to beat such hazardous risk [5-10]. Thus, it is quite necessary to develop a competent technique for the removal of toxic chemicals and dyes from the aqueous media by employing a sustainable approach [11-15].

Hence, it is essential to build up an equipped system/technique for the removal of poisonous dyes from the aqueous medium by utilizing a supportable approach. Adsorption is notable amongst the most examined methods for dye removal essentially because of its simplicity and high level of effectiveness [16].

Being a high surface/volume ratio, the nanomaterials have higher adsorption capacity and are preferred for adsorption of dye, metals and other components. [17-20].

In this article, we put our push to examine the adsorption of EBT dye (Table 1) on the surface of AlTiPbO Nanoparticles (ATPO-NPs). ATPO-NPs of the normal size of 28 nm have been synthesized by a co-precipitation strategy utilizing Titanium Oxide (TiO_2), Aluminum oxide (Al_2O_3) and Lead acetic acid derivation ($C_4H_6O_4Pb.3H_2O$) as a precursor. ATPO-NPs were described by SEM, Fourier transform infrared, X-ray diffraction and EDX. In this examination, we displayed the adsorption conduct of EBT dye, specifically containing the (-OH) hydroxyl groups. In this, we report the redesigned and perfect adsorption of EBT on ATPO-NPs. The impact of different parameters, for example, solution pH, agitation time, initial ATPO-NPs and dye concentration was studied. The adsorption procedure was additionally depicted by kinetic and isotherm investigation. [17-20]

EXPERIMENTAL METHODS

Materials

Titanium Oxide (TiO_2), Aluminum oxide (Al_2O_3) and Lead acetate ($C_4H_6O_4Pb.3H_2O$) were used as a source of Ti, Al and Pb respectively, NaOH used as a base in the synthesis of ATPO-NPs. EBT and all other reagents utilized in this examination were of an analytical grade.

Instrumentation

The Size of the ATPO-NPs was measured by FESEM (Bruker S-4800 instrument) using 15 kV acceleration voltages. Elemental percent composition was measured using the FESEM instrument (PM Image Size: 500 x 375Mag:40000×HV: 15.0 kV). X-ray (XRD) pattern was recorded by an X-ray diffractometer (Bruker D8-advance, Cu Kα k = 1.54056 nm) for 2θ values over 10-70°. An IR band (500-4000 cm^{-1}) of the adsorbent was recorded using FTIR (Model: Bruker). The EBT dye concentration in the experimental solution was determined according to conventional spectrophotometric method using UV-Visible spectrophotometer (model UV-1800) at a wavelength of 531 nm while a pH meter (Equip-Tronic EQ 610) was used for the measurement of pH.

Table 1: Chemical structure of the model EBT dye [21]

			Physical characters		
Dye	**IUPAC name**	**Structure**	**M_{wt}**	**pKa**	**Solubility (mg/l)**
Eriochrome Black T (EBT)	Naphthalenesulfonic acid, 3-hydroxy-4-[(1-hydroxy-2-naphthyl)azo]-7-nitro-sodium salt	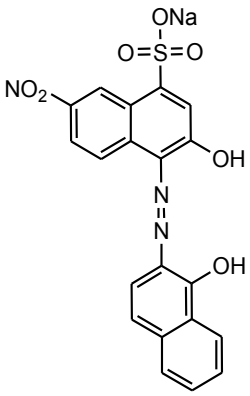	461.37	6.2, 11.55	20×10^3

Analysis Technique

Spectrophotometric method

A standard solution of dye was prepared by EBT powder. Solutions were scanned in the range of 400-700 nm and the wavelength of maximum absorption for EBT dye was determined. The accurate volume of the EBT stock solution was transferred into 25 mL flasks and diluted up to mark with the corresponding solvent to make various concentration solutions. The calibration curve for compound was obtained by plotting absorbance at the λ_{max} of dye against concentration (λ_{max} for EBT is 531 nm).

Preparation of ATPO-NPs Via Co-Precipitation

The chemical co-precipitation method was employed to synthesize the ATPO-NPs. Titanium Oxide (TiO_2), Aluminum oxide (Al_2O_3) and Lead acetate ($C_4H_6O_4Pb.3H_2O$) (molar ratio, 1:1:3) dissolved in 200-250 mL D/W and stirred for 15-20 min. NaOH solution (30 g %) dropwise was added with vigorous stirring until a dark-colored precipitate was formed. The reaction requires up to 2 hours of stirring with heating at 40 °C for complete precipitation. The precipitate was cooled down to the ambient temperature, mechanically decanted and washed several times with water followed by calcination at 90 °C for 4 hrs. After drying, the precipitate is crushed and fine powder is prepared.

Dye Adsorption Experiments

Experimental design

Basic data on the behavior of the adsorbent used are provided in batch experimentation and thus are required by all adsorption studies. These techniques are widely used to describe the capacity for adsorption, the adsorption kinetics, and the process of thermochemistry. It is easy to replicate the test protocol used. The solution and the adsorbent are intimately mixed into an agitated contacting flask for a set time to allow the system to approach equilibrium and filter the thin slurry to separate the adsorbent from the solution. Batch studies are aware that the solid/liquid interface adsorption phenomenon leads to a change in the solution's concentration. Adsorption isotherms are developed by measuring adsorbate concentration in the medium at a fixed temperature before and after the adsorption [3b, 4b].

A preliminary study carried out to optimize the agitation time needed to gain equilibrium. 0.05 g/l of ATPO-NPs were added into 50 mL dye solution of initial concentration (10 mg L^{-1}) at neutral pH and shaken with 250 rpm. After defined time intervals, the sample was removed and the absorbance of dye left in the supernatant solution after centrifugation was determined by using UV-VIS Spectrophotometry. The consistent adsorption ability of dye over nanoparticles was calculated by using the following equation.

$$\text{Adsorption Efficiency (\%)} = C_0\text{-}C_t/C_0 \times 100 \qquad (1)$$

Where, C_0 = initial dye concentration (mg/L),
C_t = concentration of dye at time t (mg/L),

The influence of pH on EBT dye removal was investigated using 10 mg/l of dye solution over a pH range of 2-8. The pH was attuned by adding 0.1 M HCl or 0.1 M NaOH solution. To the above pH-adjusted dye solution, 0.05 g/l adsorbent was added and shaken for 90 min at 25 °C.

To study the effluence of concentration of adsorbent, 0.05-0.20 g L^{-1} of ATPO-NPs were added into 50 mL dye solution (10 mg/l) with an agitation time of 90 min. The pH was adjusted to pH 2.0. Adsorption capacities were then determined for each adsorbent concentration to determine the optimal concentration of adsorbent that cause complete dye removal.

Study of Adsorption isotherms

The isothermic equilibrium of the adsorption can be depicted by plotting the contaminant concentration in the solid phase versus the liquid phase.

The distribution of pollutant molecules (or ions) between the fluid and the material is a measure of the equilibrium position in the adsorption process and may generally be expressed in one or more isothermal models. The form of an isotherm may be taken into consideration to predict if adsorption is "favorable" or "unfavorable." The isothermic form also offers qualitative information about nature or the interaction of the molecule-surface [3b, 4b].

Equilibrium study was conducted by shaking various initial dye concentrations ranging between 10 and 2000 mg L^{-1} separately with 0.05 g L^{-1} of adsorbent (ATPO-NPs) for 120 min at acidic pH (pH 4.0). After equilibrium, the qe (mg g^{-1}) i.e. dye amount adsorbed, was estimated and plotted against equilibrium concentration (Ce, mg L^{-1}). For plotting equilibrium curves, equilibrium concentration (Ce) was used instead of bulk concentration (C_0) as isotherm models involve Ce and qe as the X- and Y-axes coordinates, respectively.

Study of adsorption kinetics

The application of kinetic models, such as diffusion and adsorption models, makes the adsorption mechanism clear. The adsorbed molecule/ions originally migrate from the bulk of the solution to the surface of the material; the molecules spread throughout the limits to the surface of the material, then the adsorbate spreads from the ground to the inside of the particle and lastly the molecule responds with active sites [3b, 4b].

Adsorption Kinetic study was achieved by shaking dye solutions of 10, 20, 50, 100, 150 and 200 mg L^{-1} separately with 0.05, 0.10, 0.15 and 0.20 g L^{-1} of the adsorbent for altered time intermissions (2-90 min). After each time interim, the concentration of dye in solution was resolved and the measure of color adsorbed at each time interim (q_t, mg g^{-1}) was plotted against time (t, min) for kinetic modeling.

Desorption Study

Recovery of ATPO-NPs from dye-loaded ATPO-NPs was performed by conducting an adsorption experiment with a mixture of 10 mg L^{-1} dye solution and 0.20 g/l of adsorbent for 90 min. After equilibrium, the dye-loaded NPs were mechanically separated by means of centrifugation and the supernatant was measured for dye concentration to estimate the amount of dye adsorbed on adsorbent NPs. The dye-loaded NPs were then shaken separately with 50 mL methanol and 50 mL of 5% (v/v) methanol and NaOH. The supernatant solutions were assessed by UV-Vis Spectrophotometry to govern the extent of released dye. Five cycles were successively conducted.

RESULTS AND DISCUSSION

Characterization of the prepared ATPO Nanoparticles

To examine the general morphologies, the prepared material was characterized by Modern techniques. Fig. 1(a) displays the common SEM picture of ATPO-NPs which uncovered that the nanoparticles are developed in high thickness and possessing somewhat spherical shaped morphologies. The average size of the nanoparticles is 28 nm as shown in Fig. 1(a). The composition of the readied nanoparticles was analyzed by EDX spectroscopy joined with SEM (Fig. 1(b)). Few well-defined peaks are observed in the EDX spectrum which revealed that the prepared nanoparticles are composed of Al, Ti, Pb, and oxygen. No other significant peak associated with any contamination

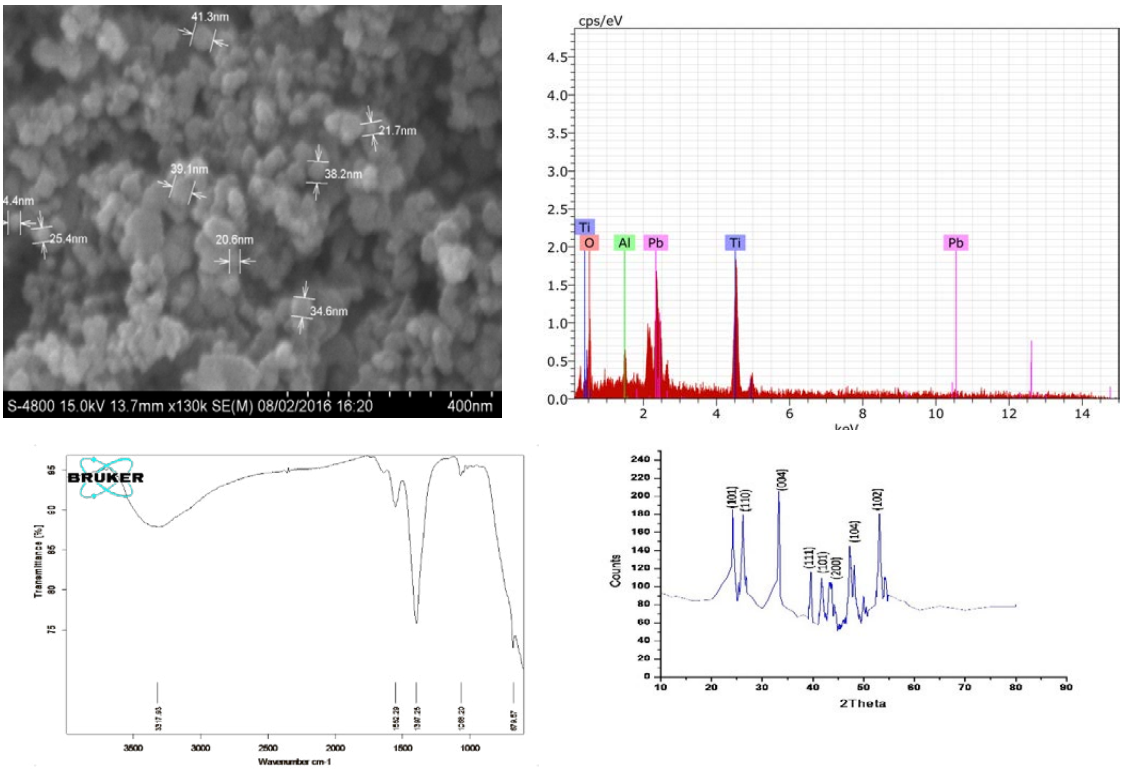

Fig. 1: (a) SEM Image and (b) EDX spectra of ATPO-NPs c) FT-IR and d) XRD Spectra of ATPO-NPs

was spotted in the EDX spectrum which confirms that the nanoparticles are mainly composed of Al, Ti, Pb, and oxygen.

FT-IR spectrum (Fig. 1c) of ATPO-NPs shows that the characteristics bands near 3317 and 1652 cm^{-1} refer to the O-H stretching vibration. X-ray diffraction (XRD) spectroscopy is a strong technology for the identification of the composition and pure phase of the samples. The crystalline structures of ATPO-NPs were studied by XRD. As shown in Fig. 1d, ATPO-NPs exhibited diffraction peaks at 24.2° (101), 26.5° (110), 32.8° (004), 39.9° (111), 41.6° (101), 44.8° (200), 47.9° (104) and 53.9° (102). These peaks indicated that ATPO-NPs was effectively formed.

Dye adsorption experiments

Effect of contact time

The impact of contact time on the adsorption of model dye EBT for instance of anionic dye was agitated to decide the time taken by 0.05 g L^{-1} ATPO-NPs to (10 mg L^{-1}) from the system at regular pH. The adsorption limit after effect of ATPO-NPs has appeared in Figs. 2 and 3. Inside the initial 60 min there was a critical increment in the adsorption limit of NPs. Further increase in the contact time was accompanied by slow increase in the adsorption capacity of NPs. The ATPO-NPs showed an adsorption capacity of 96% for EBT, after 60 min. The experiment time was extended to 90 min and it was observed that the adsorption of dye on the NPs reached equilibrium after 90 min. This may indicate that the adsorption starts very fast on the external surface followed by slower adsorption on the internal surface of the nano-composites. An agitation time of 90 min was selected for further works.

Effect of pH

The impact of pH in the range of 2–8 on the expulsion of the model dye EBT was explored with initial color (dye) concentration of 20 mg L^{-1} and 0.05 g L^{-1} adsorbent mass. As Fig. S1 appears, for the anionic dye EBT, the adsorption is high in acidic medium and declines with the expansion in solution pH. This can be ascribed to the way that as the pH is brought down, the hydroxyl groups of ATPO-NPs are protonated and the general surface

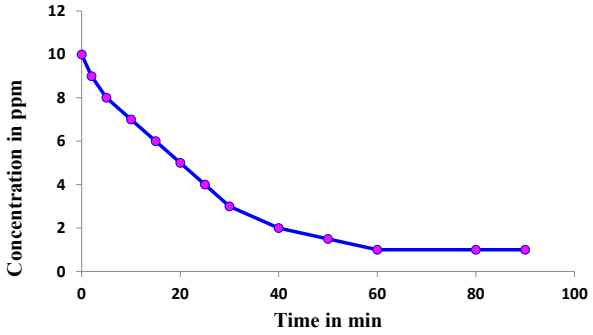

Fig. 2: Plot of concentration (ppm) Vs Time (min)

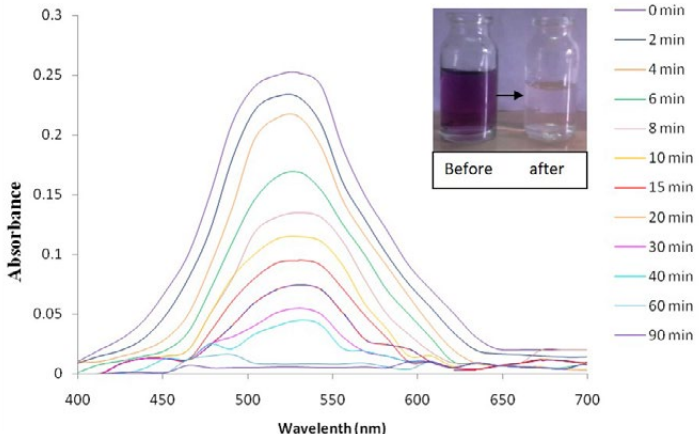

Fig. 3: Time variation study

charge on the NPs will wind up plainly positive. Such an outcome will advance response with EBT through electrostatic powers of attraction [22].

Effect of adsorbent mass

The influence of the adsorbent mass usually determines the solid adsorbent's capacity for a given initial concentration of adsorbate in a solution. Fig. 4 shows the effect of the ATPO-NPs mass on the adsorption of the model dye from the aqueous solutions. It is clear from the figure that the % of model dye removed, increasing gradually as the nanoparticles mass increased. The anionic dye % removal affirmed that 0.05 g L^{-1} of ATPO-NPs has a removal efficiency of 86 % for EBT dye. The enhancement that was observed in the % removed of model dye was principally due to the increase in the active sites on the nanoparticles available for adsorption of dye molecules. Further increase in the dosage of nanoparticles from 0.05 to 0.20 g L^{-1} was accompanied by further increase in the % dye removed to over 98 %.

Adsorption kinetic study

The contact time involves to achieve the equilibrium is an essential factor for the dye removal application by the adsorption. Thus, the time-dependent studies were also performed in the range of 0–120 min. Through detailed experiments, it was found that colorless dye solution was obtained after 90 min of equilibration time for EBT dye. The obtained data was further utilized to investigate the adsorption kinetics of the dye molecules over ATPO-NPs by employing the well defined pseudo-first-order kinetic (Supplementary Eq. 1) and pseudo-second-order kinetic model (supplementary Eq. 2) [23].

The acquired values for EBT dye in the presence of ATPO-NPs are exhibited in Fig. 5.

The determined active parameters are provided

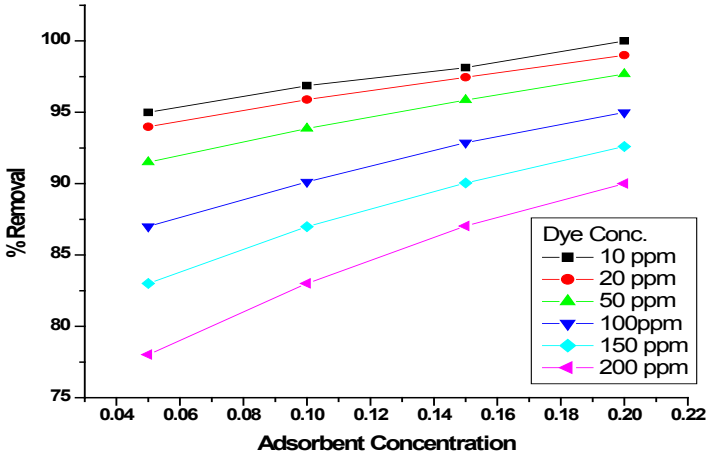

Fig. 4: Adsorbent concentration variation study

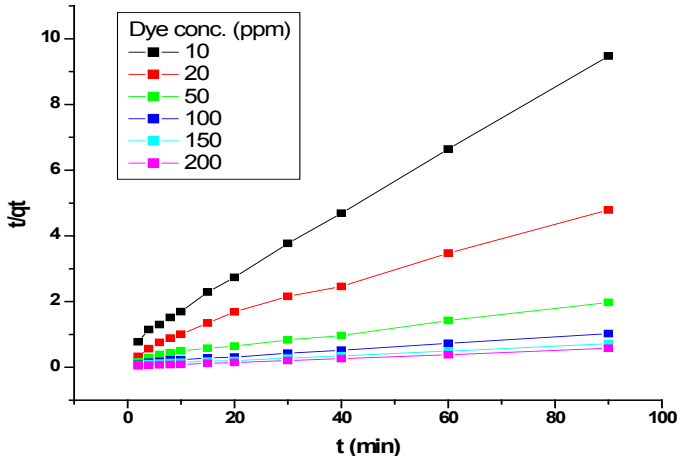

Fig. 5: Pseudo-second-order kinetics for EBT adsorption

in Table 2. The relationship coefficient for the pseudo-1st-order kinetic model is moderately low; the determined q_e value obtained from this condition does not give reasonable value. This outcome recommends that the adsorption procedure does not pursue the pseudo-first-order kinetic model. It presents a perfect fit for the second-order kinetic for adsorbent with to a great degree R^2=0.999. The best fit for the pseudo-second-order kinetic model that the adsorption mechanism relies upon the adsorbate and adsorbent.

Adsorption isotherm modeling

The adsorption limit of ATPO-NPs was determined by the adsorption isotherm. Writing uncovered different models to clarify the conduct of adsorbent materials [24]. In this present work, four diverse adsorption isotherms were utilized, to be specific; Freundlich, Langmuir, Temkin, and Dubinnin-Radushkevich (D-R) to accomplish basic data. The relating straight condition for Langmuir, Freundlich, and Temkin and D-R adsorption isotherm is communicated as in supplementary Eq. 3, 4, 5 and 7 respectively [25-29].

The calculated values of Freundlich, Langmuir, Temkin, and D-R adsorption isotherm constants are demonstrated in Table 3.

The observed results clearly revealed that the adsorption was mainly chemisorptions in nature [28-30]. Moreover, on comparing the linear correlation coefficients values obtained from different models, it was found that the Langmuir model yielded the best fit with higher R^2 values (Fig. S2) when contrasted with the other three models for the dye adsorption.

Intra-particle diffusion model

The trial information was additionally researched by the diffusion (intra-molecule) model to clarify the diffusion mechanism. The plots (q_t vs.

Table 2: Kinetic parameters of EBT adsorption onto ATPO-NPs (adsorbent dose 0.05 g/L and initial concentration 10–200 mg/L)

Models	Parameters	Initial EBT concentration (mg/L)					
		10	20	50	100	150	200
First order	$K_f \times 10^2$	0.023	0.023	0.021	0.021	0.021	0.032
kinetic	qe	1.013	1.005	1.001	1.001	1.001	1.001
	R^2	0.933	0.985	0.92	0.937	0.892	0.826
Second order	K_2	0.0127	0.0048	0.0015	0.0008	0.0007	0.0012
kinetic	qe	10.31	20.41	52.63	100	142.85	166.66
	R^2	0.999	0.989	0.991	0.995	0.996	0.998

Table 3: Various isotherm constants and their correlation coefficients calculated for the adsorption of EBT onto ATPO-NPs

Isotherm	Linear form	Parameters	
Langmuir	$C_e/q_e = C_e\alpha_L/K_L + 1/K_L$	q_{max} (mg/g)	1000
		K_L (L/mg)	8.93
		R^2	0.999
Freundlich	lnQe = 1/n 1nCe+lnkf	n	1.85
		K_f (L/mg)	18.48
		R^2	0.914
Temkin	qe = Bl ln KT + Bl ln Ce	B_1	0.012
		K_T (L/mg)	1.1273E+31
		R^2	0.947
Dubinin–Radushkevich	$lnqe = lnQs - B\varepsilon^2$	Qs (mg.g)	257.49
(D-R)		B	0.000001
		E (KJ/mol)	707.11
		R^2	0.744

$t^{0.5}$) represent multi-linearity, which indicates two or more steps occurring in the adsorption process. The relationship between q_t vs. $t^{0.5}$ is plotted in Fig. 6. The intra-molecule dispersion constant and the limit layer thickness was calculated using the linear supplementary Eq. 10 (Table 4).

If the plot (q_t versus $t^{1/2}$) is a straight line going from origin, indicate that intra-molecule dissemination moves towards becoming rate-controlling step. As seen from Fig. 7 the plot isn't straight over the entire time extend which implies that the intraparticle dispersion isn't the

Table 4: Obtained values of Intra-particle diffusion model parameters

Parameters	Nanoparticle concentration (mg)			
	50	100	150	200
K_{id1}	36.14	36.58	37.18	36.88
C_1	4.196	1.097	15.17	30.66
R^2	0.986	0.973	0.946	0.994
K_{id2}	5.037	4.531	4.197	4.57
C_2	113.7	126.4	134.8	140.3
R^2	0.731	0.837	0.904	0.906

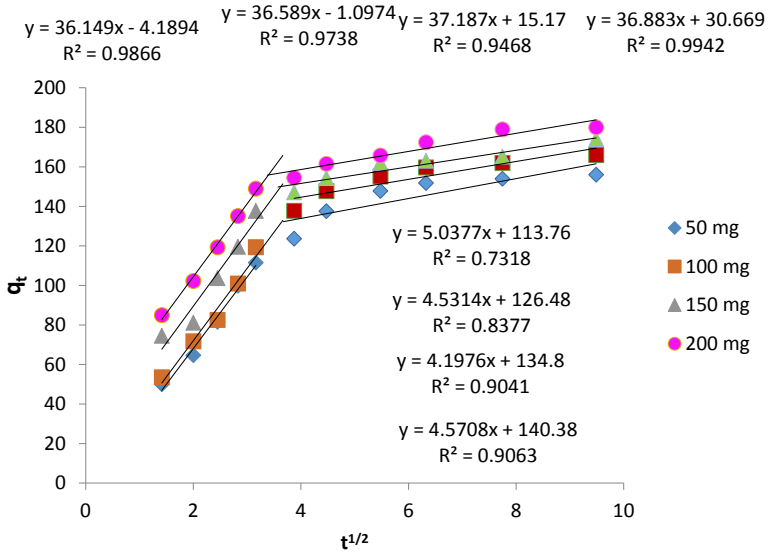

Fig. 6: Intra-particle diffusion plots for adsorption of EBT on ATPO-NPs

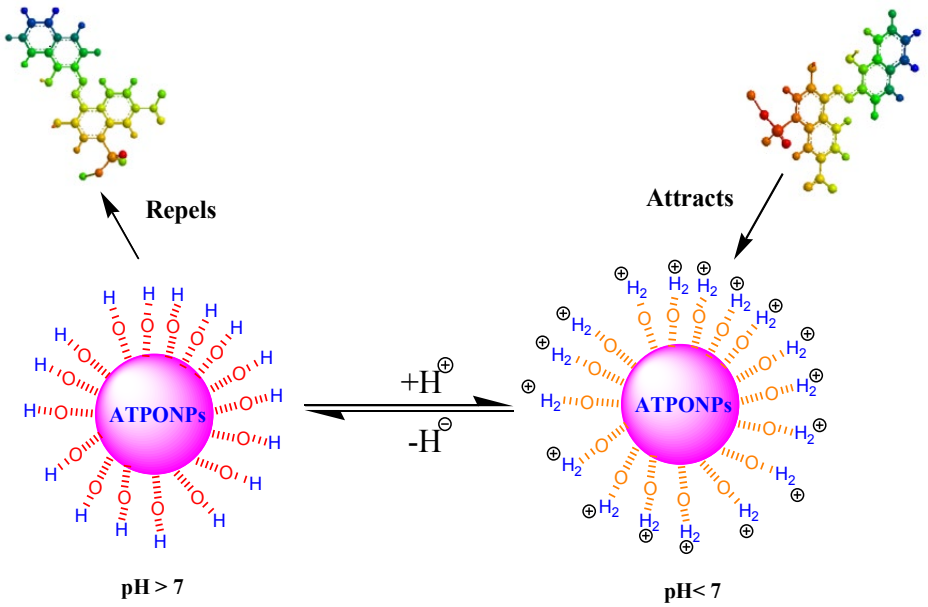

Fig. 7: Schematic representation of electrostatic interaction between protonated (ATPO-NPs) adsorbent surface and EBT dye.

rate deciding step of the adsorption mechanism of the model dye on ATPO-NPs. The estimations of intercept (Table 4) give a thought regarding the limit layer thickness, i.e., larger the intercept more prominent is the limit layer impact and this means that the adsorption is more boundary layer controlled [31, 32].

Mechanism of the adsorption

The ATPO-NP surfaces are largely secured with hydroxyl groups, which fluctuate as per the shapes at various pH. The surface charge is neutral at pHzpc (the pH estimation of the zero point charge, pHzpc, of the ATPONPs are roughly 4.9).

Under the pHzpc, the adsorbent surface is positively charged and anionic dye adsorption happens. This marvel has been seen with the anionic dye-EBT. Step by step, as the pH of the system builds, a corresponding lessening in adsorption happened because of the progressive deprotonation of the hydroxyl bunches in the adsorbent and the electrostatic release between the contrarily charged particles in the adsorbent and the shading anions. There was likewise opposition between OH^- anions (high pH) and anionic dye for positively charged adsorption destinations. The sub-atomic size and number of anionic groups (SO_3^{2-}) on the dye particle are likewise critical elements for their diverse adsorption conduct. For instance, EBT indicated higher adsorption because of higher sub-atomic size; notwithstanding the nearness of a sulphonate a mass in EBT, giving the EBT surface more electronegative, prompting greater adsorption on the surface of positively charged NPs [33].

The pH of the system assumes an essential part in the adsorption procedure as the surface restricting sites of the adsorbent change with an adjustment in pH values. Evacuation of EBT decreased with increasing pH and the most extreme value was seen at pH 2.0. The hydroxyl groups in ATPONPs, as appeared in the FT-IR range (Fig. 1c, crest at 3317.93 cm^{-1}) assume an overwhelming part in EBT adsorption. Contingent upon the pH estimation of the solution, the adsorption surface is subjected to protonation or deprotonation as represented by equation 12:

$$-\text{Al-Ti-Pb-O-H} + H^+ \leftrightarrows -\text{Al-Ti-Pb-O-H}_2 \qquad (2)$$

At pH<7, -Al-Ti-Pb-O-H_2 is the dominant species. These species having high positive charge thickness make the negatively charged dye (EBT) adsorption ideal because of electrostatic fascination. However, at pH>7, -Al-Ti-Pb-O-H is the dominant species in ATPO-NPs (Fig. 7). Such deprotonated species undergo electrostatic repulsion for negatively charged dye. This causes decreased dye adsorption [34].

Table 5: Comparison of maximum adsorption capacities (q_{max}, mg/g) of some adsorbents for EBT from the aqueous phase

Adsorbent	qm(mg/g)	References
Iron Oxide Nanoparticles	250.1	[1]
Eucalyptus bark	52.37	[36]
Scolymus hispanicus L.	120.42	[41]
Activated carbon	160.4	[40]
Nteje clay	16.26	[42]
$NiFe_2O_4$	47	[37]
MnO_2-Coated Zeolite	12.35	[38]
magnetite/silica/pectin NPs	80.15	[32]
magnetite/pectin NPs	103.41	[32]
Hydrophobic cross-linked polyzwitterionic acid (HCPZA)	15.9	[23]
GO- Fe_3O_4	147.25	[33]
Calcined MgAl-LDH	540.91	[21]
Calcined CoAl-LDH	419.87	[21]
Calcined NiFe-LDH	132.49	[21]
ATPO-NPs	1000	Present Study

Thermodynamic studies

Assessment of temperature was done with the extent of testing the capacity of ATPO-NPs in dye removal in various conditions. Information was gathered at three temperatures: from 298 to 308 K. The model dye adsorbed on ATPO-NPs as the capacity of system temperature has appeared in Fig. S3. An expansion of the measure of dye adsorbed was seen when the temperature increases. From these outcomes, thermodynamic parameters incorporating the change in free energy (ΔG°), enthalpy (ΔH°) and entropy (ΔS°) were utilized to represent thermodynamic behaviour of the adsorption of the model dye onto ATPO-NPs. These parameters were calculated using the supplementary Eq. 11, 12 and 13:

The change in enthalpy (ΔH°) and entropy change (ΔS°) of adsorption were evaluated from the intercept of the plot of ln K versus 1/T yields, individually.

The calculated ΔG° estimations of this adsorption procedure are -5.42, -5.79 and -6.17 KJ/mol for 298, 308 and 318 K temperature respectively, and these characteristics confirm that adsorption at lower temperatures was spontaneous, feasible and more perfect. The positive estimations of ΔH° (57.37 KJ/mol) for the considered scope of temperature support the endothermic nature of the procedure. The change in entropy (ΔS°) is 37.45 (J/mol.K) relates to the increased disorder and randomness at the solid-solution interface during the adsorption of dye on the adsorbents [35].

The increased mobility of the large color ion at temperature can also be attributed to the improvement in the adsorption capacity of ATPO NPs. More and more molecules can also obtain enough energy to interact with the surface at active sites.

Real sample analyses

Furthermore, the prepared nanoparticles were used to check the adsorbent efficiency in actual water samples collected from the industry outlet. Dissolving the concentration of dye solution to 30 ppm and produced the spiked samples (S1, S2, and S3). ATPO NPs feasibility has been tested by calculating the removal efficiency on each system for all the prepared samples using optimized conditions. The results showed that more than 89% of the dye molecules were removed from each of the spiked water samples. Thus, the results observed confirmed that simply prepared nanoparticles efficiently remove toxic chemicals and dye from wastewater. [36].

DESORPTION AND REGENERATION STUDIES

Dye adsorption on the surface of ATPO-NPs is a reversible procedure. With the goal that ATPO-NPs can be reused by doing desorption of dye from the dye loaded adsorbent. Four dissolvable frameworks including methanol, 1:1 mixture of 0.1 mol/L NaOH and methanol, and propanol were chosen to elute EBT from the surface of ATPO-NPs. The higher desorption proficiency was acquired utilizing 5.0 mL of 1:1 mixture of 0.1 mol/L NaOH and methanol in examination with different eluents. To evaluate the reuse capacity of adsorbent, a few adsorptions/desorption cycles were completed (Fig. S5). After every adsorption cycle, the color was eluted from the surface of ATPO-NPs utilizing 5.0 mL of 1:1 mixture of 0.1 mol/L NaOH and methanol, this is rehashed for 5 times and afterward ATPO-NPs reused for resulting adsorption of EBT dye. The got result unmistakably demonstrated that over 90% of EBT can be expelled from the aqueous phase by the recovered ATPO-NPs got after 5 cycles of adsorption/desorption.

CONCLUSION

The nanostructure material created by a solitary way, i.e. straightforward co-precipitation process and its size affirmed by the property assessment uncovered that the material had a nanostructure sort with a normal size of 28 nm existing together with little grains. What's more, ATPO-NP has been utilized to expel EBT from fluid media requiring little to no effort. The outcomes demonstrated that ATPO-NP can be utilized as a powerful adsorbent to remove EBT from a solution. The measure of adsorbed dye differed with the underlying pH, the contact time and the EBT concentration. The best pH for adsorption was 2.0. The adsorption equilibrium of the dye was come to following an hour and the greatest adsorption limit obtained is 1000 mg/g of dye for 0.2 g of ATPO-NP. The outcomes demonstrated that the incorporated nanoparticles could viably remove high concentration of EBT dye in short contact time. The isothermal model uncovered that the Langmuir condition depicts well the adsorption of the EBT dye to the ATPO NPs. Pseudo-Second order kinetic rate of adsorption is found. Contrasted and different sponges, nanoparticles have high adsorption proficiency, as well as are promptly arranged for reuse. Because

of the high surface region and molecule estimate at the nanoscale, ATPO-NP demonstrated good adsorption capacity for EBT. ATPO NPs can be created in a straightforward and practical route for different modern applications. The synthesized ATPO-NPs can be very much scattered in water and can be promptly isolated from the medium after adsorption. These special nanostructures could be utilized as a promising adsorbent option for removal of contaminants from industrial wastewater.

ACKNOWLEDGMENTS

This work was financially supported by the Council of Scientific & Industrial Research (CSIR) [Ack. No.122066/2K17/1]. The authors are grateful and thankful to the Council of Scientific & Industrial Research (CSIR), India.

CONFLICTS OF INTEREST

There are no conflicts to declare.

REFERENCES

1. Saha B, Das S, Saikia J, Das G. Preferential and Enhanced Adsorption of Different Dyes on Iron Oxide Nanoparticles: A Comparative Study. The Journal of Physical Chemistry C. 2011;115(16):8024-33.
2. May-Lozano M, Mendoza-Escamilla V, Rojas-García E, López-Medina R, Rivadeneyra-Romero G, Martinez-Delgadillo SA. Sonophotocatalytic degradation of Orange II dye using low cost photocatalyst. Journal of Cleaner Production. 2017;148:836-44.
3. Daneshvar E, Vazirzadeh A, Niazi A, Kousha M, Naushad M, Bhatnagar A. Desorption of Methylene blue dye from brown macroalga: Effects of operating parameters, isotherm study and kinetic modeling. Journal of Cleaner Production. 2017;152:443-53.
4. a) Keqing Zhou, Qiangjun Zhang, Biao Wang, Jiajia Liu, Panyue Wen, Zhou Gui and Yuan Hu, The integrated utilization of typical clays in removal of organic dyes and polymer nanocomposites, Journal of Cleaner Production, 81 (2014) 281-289. b) Morin-Crini N, Winterton P, Fourmentin S, Wilson LD, Fenyvesi E, Crini G, Water-insoluble β-cyclodextrin-epichlorohydrin polymers for removal of pollutants from aqueous solutions by sorption processes using batch studies: a review of inclusion mechanism. Prog Polym Sci 78 (2018) 1–23.
5. Lee LY, Gan S, Yin Tan MS, Lim SS, Lee XJ, Lam YF. Effective removal of Acid Blue 113 dye using overripe Cucumis sativus peel as an eco-friendly biosorbent from agricultural residue. Journal of Cleaner Production. 2016;113:194-203.
6. Turcanu A, Bechtold T. Cathodic decolourisation of reactive dyes in model effluents released from textile dyeing. Journal of Cleaner Production. 2017;142:1397-405.
7. Sahraei R, Sekhavat Pour Z, Ghaemy M. Novel magnetic bio-sorbent hydrogel beads based on modified gum tragacanth/ graphene oxide: Removal of heavy metals and dyes from water. Journal of Cleaner Production. 2017;142:2973-84.
8. Markandeya, Dhiman N, Shukla SP, Kisku GC. Statistical optimization of process parameters for removal of dyes from wastewater on chitosan cenospheres nanocomposite using response surface methodology. Journal of Cleaner Production. 2017;149:597-606.
9. Bagheri AR, Ghaedi M, Asfaram A, Hajati S, Ghaedi AM, Bazrafshan A, et al. Modeling and optimization of simultaneous removal of ternary dyes onto copper sulfide nanoparticles loaded on activated carbon using second-derivative spectrophotometry. Journal of the Taiwan Institute of Chemical Engineers. 2016;65:212-24.
10. Asfaram A, Ghaedi M, Hajati S, Goudarzi A. Synthesis of magnetic γ-Fe 2 O 3 -based nanomaterial for ultrasonic assisted dyes adsorption: Modeling and optimization. Ultrasonics Sonochemistry. 2016;32:418-31.
11. Dastkhoon M, Ghaedi M, Asfaram A, Goudarzi A, Mohammadi SM, Wang S. Improved adsorption performance of nanostructured composite by ultrasonic wave: Optimization through response surface methodology, isotherm and kinetic studies. Ultrasonics Sonochemistry. 2017;37:94-105.
12. Saravanan R, Karthikeyan S, Gupta VK, Sekaran G, Narayanan V, Stephen A. Enhanced photocatalytic activity of ZnO/CuO nanocomposite for the degradation of textile dye on visible light illumination. Materials Science and Engineering: C. 2013;33(1):91-8.
13. Saravanan R, Gupta VK, Narayanan V, Stephen A. Visible light degradation of textile effluent using novel catalyst ZnO/γ-Mn2O3. Journal of the Taiwan Institute of Chemical Engineers. 2014;45(4):1910-7.
14. Saravanan R, Gupta VK, Mosquera E, Gracia F, Narayanan V, Stephen A. Visible light induced degradation of methyl orange using β-Ag0.333V2O5 nanorod catalysts by facile thermal decomposition method. Journal of Saudi Chemical Society. 2015;19(5):521-7.
15. Ghaedi M, Hajati S, Zaree M, Shajaripour Y, Asfaram A, Purkait MK. Removal of methyl orange by multiwall carbon nanotube accelerated by ultrasound devise: Optimized experimental design. Advanced Powder Technology. 2015;26(4):1087-93.
16. Dastkhoon M, Ghaedi M, Asfaram A, Goudarzi A, Langroodi SM, Tyagi I, et al. Ultrasound assisted adsorption of malachite green dye onto ZnS:Cu-NP-AC: Equilibrium isotherms and kinetic studies – Response surface optimization. Separation and Purification Technology. 2015;156:780-8.
17. a) M. Ghaedi, S. Hajati, M. Zaree, Y. Shajaripour, A. Asfaram, M.K. Purkait, Removal of methyl orange by multiwall carbon nanotube accelerated by ultrasound devise: Optimized experimental design, Advanced Powder Technology, 26 (2015) 1087–1093. b) Ganesh Jethave, Umesh Fegade, Sanjay Attarde, Sopan Ingle, Facile synthesis of Lead Doped Zinc-Aluminum Oxide Nanoparticles (LD-ZAO-NPs) for efficient adsorption of anionic dye: Kinetic, isotherm and thermodynamic behaviors, Journal of Industrial and Engineering Chemistry 53 (2017) 294–306.
18. a) Vinod K. Gupta, Shilpi Agarwal, Tawfik A. Saleh, Synthesis and characterization of aluminacoated carbon

nanotubes and their application for lead removal, Journal of Hazardous Materials, 185 (2011) 17–23. b) Umesh Fegade, Ganesh Jethave, Kang-Yang Su, Wei-Ru Huang, Ren-Jang Wu, An Multifunction $Zn_{0.3}Mn_{0.4}O_4$ Nanospheres for Carbon dioxide Reduction to Methane via Photocatalysis and Reused after fifth cycles for Phosphate Adsorption, Journal of Environmental Chemical Engineering, (2018).

19. a) Tawfik A. Saleh & Vinod K. Gupta, Column with CNT/ magnesium oxide composite for lead(II) removal from water, Environ Sci Pollut Res, 19 (2012) 1224–1228. b) Ganesh Jethave, Umesh Fegade, Design and synthesis of $Zn_{0.3}Fe_{0.45}O_3$ nanoparticle for efficient removal of Congo red dye and its kinetic and isotherm investigation, International Journal of Industrial Chemistry, 9 (2018) 85–97.
20. a) Arash Asfaram, Mehrorang Ghaedi, Alireza Goudarzi, Maryam Rajabi, Response surface methodology approach for optimization of simultaneous dyes and metal ions ultrasoundassisted adsorption onto Mn doped Fe_3O_4-NPs loaded on AC: Kinetic and isotherm study, Dalton Trans, 44 (2015) 14707-14723. b) Ganesh Jethave, Umesh Fegade, Rahul Rathod and Jagdish Pawar, Dye Pollutants removal from Waste water using Metal Oxide Nanoparticle embedded Activated Carbon: An Immobilization study, journal of dispersion science and technology, (2018) 1-11.
21. Zubair M, Jarrah N, Manzar MS, Al-Harthi M, Daud M, Mu'azu ND, et al. Adsorption of eriochrome black T from aqueous phase on MgAl-, CoAl- and NiFe- calcined layered double hydroxides: Kinetic, equilibrium and thermodynamic studies. Journal of Molecular Liquids. 2017;230:344-52.
22. Bhowmik KL, Debnath A, Nath RK, Das S, Chattopadhyay KK, Saha B. Synthesis and characterization of mixed phase manganese ferrite and hausmannite magnetic nanoparticle as potential adsorbent for methyl orange from aqueous media: Artificial neural network modeling. Journal of Molecular Liquids. 2016;219:1010-22.
23. Saleh TA, Muhammad AM, Ali SA. Synthesis of hydrophobic cross-linked polyzwitterionic acid for simultaneous sorption of Eriochrome black T and chromium ions from binary hazardous waters. Journal of Colloid and Interface Science. 2016;468:324-33.
24. Kyzas GZ, Matis KA. Nanoadsorbents for pollutants removal: A review. Journal of Molecular Liquids. 2015;203:159-68.
25. Langmuir I. THE CONSTITUTION AND FUNDAMENTAL PROPERTIES OF SOLIDS AND LIQUIDS. PART I. SOLIDS. Journal of the American Chemical Society. 1916;38(11):2221-95.
26. H.M.F. Freundlich, Zeit. Phys. Chem. 57 (1906) 385–470.
27. M.J. Temkin, V. Pyzhev, Acta Physiochim. USSR 12 (1940) 217–222.
28. M.M. Dubinin, Chem. Rev. 60 (1960) 235–266.
29. M.M. Dubinin, Zh. Fiz. Khim. 39 (1965) 1305–1317.
30. L.V. Radushkevich, Zh. Fiz. Khim. 20 (1949) 1410–1420.
31. Weber TW, Chakravorti RK. Pore and solid diffusion models for fixed-bed adsorbers. AIChE Journal. 1974;20(2):228-38.
32. Attallah OA, Al-Ghobashy MA, Nebsen M, Salem MY. Removal of cationic and anionic dyes from aqueous solution with magnetite/pectin and magnetite/silica/pectin hybrid nanocomposites: kinetic, isotherm and mechanism analysis. RSC Advances. 2016;6(14):11461-80.
33. Raghu MS, Yogesh Kumar K, Prashanth MK, Prasanna BP, Vinuth R, Pradeep Kumar CB. Adsorption and antimicrobial studies of chemically bonded magnetic graphene oxide-Fe 3 O 4 nanocomposite for water purification. Journal of Water Process Engineering. 2017;17:22-31.
34. Moeinpour F, Alimoradi A, Kazemi M. Efficient removal of Eriochrome black-T from aqueous solution using NiFe2O4 magnetic nanoparticles. Journal of Environmental Health Science and Engineering. 2014;12(1).
35. Chaudhary S, Kaur Y, Umar A, Chaudhary GR. 1-butyl-3-methylimidazolium tetrafluoroborate functionalized ZnO nanoparticles for removal of toxic organic dyes. Journal of Molecular Liquids. 2016;220:1013-21.
36. P. Dave, S. Kaur and E. Khosla, removal of Eriochrome black-T by adsorption on to eucalyptuse bark using green technology, Indian J. Chem. Technol., 18 (2011) 53–60.
37. Moeinpour F, Alimoradi A, Kazemi M. Efficient removal of Eriochrome black-T from aqueous solution using NiFe2O4 magnetic nanoparticles. Journal of Environmental Health Science and Engineering. 2014;12(1).
38. Aguila DMM, Ligaray MV. Adsorption of Eriochrome Black T on MnO2-Coated Zeolite. International Journal of Environmental Science and Development. 2015;6(11):824-7.
39. Jethave G, Fegade U, Attarde S, Ingle S. Facile synthesis of Lead Doped Zinc-Aluminum Oxide Nanoparticles (LD-ZAO-NPs) for efficient adsorption of anionic dye: Kinetic, isotherm and thermodynamic behaviors. Journal of Industrial and Engineering Chemistry. 2017;53:294-306.
40. de Luna MDG, Flores ED, Genuino DAD, Futalan CM, Wan M-W. Adsorption of Eriochrome Black T (EBT) dye using activated carbon prepared from waste rice hulls—Optimization, isotherm and kinetic studies. Journal of the Taiwan Institute of Chemical Engineers. 2013;44(4):646-53.
41. Barka N, Abdennouri M, Makhfouk MEL. Removal of Methylene Blue and Eriochrome Black T from aqueous solutions by biosorption on Scolymus hispanicus L.: Kinetics, equilibrium and thermodynamics. Journal of the Taiwan Institute of Chemical Engineers. 2011;42(2):320-6.
42. Elijah O, T N. Adsorption studies on the removal of Eriochrome black-T from aqueous solution using Nteje clay. SOP Transactions on Applied Chemistry. 2014;1(2):14-25.